Available online at www.sciencedirect.com

ScienceDirect

Ceramics International 40 (2014) 1781–1788

CERAMICS INTERNATIONAL

www.elsevier.com/locate/ceramint

Effect of grain size on the electrical properties of high dense BPT nanocrystalline ferroelectric ceramics

Venkata Ramana Mudinepalli[a], Shenhua Song[a,*], Junqin Li[b], B.S. Murty[c]

[a]*Shenzhen Key Laboratory of Advanced Materials, Department of Materials Science and Engineering, Shenzhen Graduate School, Harbin Institute of Technology, Shenzhen 518 055, China*

[b]*College of Materials Science and Engineering, Shenzhen University, Shenzhen 518060, China*

[c]*Department of Metallurgical and Materials Engineering, Indian Institute of Technology Madras, Chennai 600036, India*

Received 29 March 2013; received in revised form 15 July 2013; accepted 16 July 2013
Available online 24 July 2013

Abstract

Nanosized $Ba_{0.8}Pb_{0.2}TiO_3$ powders obtained by high energy ball milling were compacted and sintered into nanocrystalline ferroelectric ceramics using spark plasma sintering (SPS). The prepared ceramic samples were characterized by field emission scanning electron microscopy, X-ray diffraction, and electrical property measurements. All the samples show a density over 97% of the theoretical value and an average grain size of ~60–200 nm depending on the ball milling time. The dielectric data exhibit a ferroelectric–paraelectric phase transition and a maximum relative permittivity of 19,000 at 225 °C and 100 kHz at the average grain size of ~60 nm. The values of the dielectric constants both at room temperature and at the phase transition temperature increase considerably as the average grain size decreases. The remanent polarization and coercive field strength decrease slightly as the average grain size decreases but remain at an acceptable level for ferroelectric applications.

Keywords: A. Sintering; B. Grain size; C. Electrical properties; D. Perovskites

1. Introduction

Miniaturization of ferroelectric components is of considerable interest in the microelectronic industry. Recent advances in solid state science have enabled the fabrication of ferroelectric materials and devices with nanostructures [1,2]. Piezoelectric barium titanate ($BaTiO_3$) is a well-known ferroelectric material with a high permittivity at room temperature and is used in the manufacture of thermistors, multilayer capacitors and electro-optic devices [3]. There are four possible crystal structures (rhombohedral, orthorhombic, tetragonal and cubic) that occur for $BaTiO_3$ between −100 and 135 °C and these structural phase transitions induce large variations in permittivity and dielectric loss. In order to avoid these disadvantages, doped materials are used. For example, Nb and Co are commonly added to $BaTiO_3$ to stabilize the permittivity and reduce the dielectric loss [4]. An investigation was made regarding the effect on the dielectric properties of $BaTiO_3$ containing a small percentage of Pb, and results showed a ferroelectric Curie temperature increase from 120 °C to 225 °C [5,6]. As shown recently [7,8], the interest in Pb-based materials has decreased due to its toxicity. However, Pb-modified $BaTiO_3$ ferroelectric ceramics are still investigated for applications in many types of electronic devices, such as transducers, actuators, sensors, hydrophones, electro-optical modulators, infrared sensors and piezoelectric actuators, especially for high frequency and high temperature applications [6,9]. These ferroelectric materials are usually prepared by conventional methods, which require high temperature and long reaction times and result in an inhomogeneous particle size distribution making them unsuitable for high performance ceramics. Also, with the miniaturization of electronic devices, it becomes increasingly important to investigate the size effects on the ferroelectric properties when approaching the nanoscale. It will require powders with controlled stoichiometry and small and uniform particle size to achieve this goal.

Spark plasma sintering (SPS) is a newly developed synthesis and processing technique which allows sintering and sinter-bonding at relatively low temperatures and over a short

*Corresponding author. Tel.: +86 755 26033465; fax: +86 755 26033504.
E-mail addresses: shsong@hitsz.edu.cn, shsonguk@aliyun.com (S. Song).

0272-8842/$ - see front matter © 2013 Elsevier Ltd and Techna Group S.r.l. All rights reserved.
http://dx.doi.org/10.1016/j.ceramint.2013.07.078

period of time by charging the gaps between powder particles with electrical energy to generate the spark plasma. SPS systems generally apply pressure to the sample but offer many advantages over systems using heat and pressure, such as hot press (HP) sintering, hot isostatic pressing (HIP) and high pressure furnaces. The advantages include ease of operation, accurate control of sintering energy, high sintering speed, and high reproducibility, safety and reliability. The SPS temperature is at least 300 °C lower than that used in conventional sintering [10,11], and even lower than that used in hot pressing [12], because of the SPS-assisted densification effect. The main difference between SPS and other sintering methods using heat and pressure is that SPS is a process which makes use of microscopic electrical discharge between particles under pressure. Material processing (pressure, temperature rise and holding time) is completed in 5–20 min. The relatively low processing temperature, combined with short processing times, ensures control over grain growth and final microstructure.

It is well known [13] that the grain size (GS) has a dramatic influence on the properties of ferroelectric materials. Although SPS is commonly used to produce dense metal and engineering ceramics, there are relatively few reports on the application of this technique to produce dense ceramics for electrical applications. In the present work, high energy ball milling followed by SPS has been used to prepare nanocrystalline $Ba_{0.8}Pb_{0.2}TiO_3$ (abbreviated as BPT) ceramics. BPT has a relatively high Curie transition temperature (around 225 °C), which is appropriate for use in electronic devices at high frequencies and temperatures. We report on the densities and grain sizes of the SPS-prepared ferroelectric BPT ceramics and the effect of these on the electrical properties.

2. Experimental procedure

2.1. Sample preparation

High pure chemicals (≥99%, Alfa Aesar, USA) of $BaCO_3$, PbO and TiO_2 were weighed and mixed to give a final composition of $Ba_{0.8}Pb_{0.2}TiO_3$. In order to obtain different grain sizes after SPS at the same conditions of temperature, pressure and time, a pre-sintering powder was obtained by high energy ball milling using a Fritsch P5 (Fritsch GmbH, Germany) high-energy planetary ball mill with WC jars and balls. The ball milling was done for times between 10 and 40 h which allowed pre-sintering particles to be different in size.

Ball milled powders were then sintered in the form of disks using spark plasma sintering. A schematic diagram of the SPS apparatus is shown in Fig. 1. Between the powder and the inner surface of the 10 cm diameter die, a graphite foil (0.15 μm) was placed in order to facilitate sample extraction after the SPS process. The die was then placed inside the reaction chamber of the SPS apparatus and the system was evacuated (10 Pa). A mechanical pressure of 48 MPa was then applied through the plungers and a pulsed electrical current of 800 A was set. The compacted powder was heated at a rate of 200 °C/min to 900 °C and held for 5 min, and then the

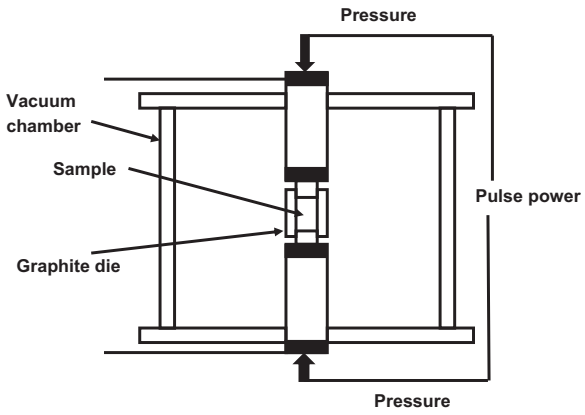

Fig. 1. Schematic diagram of the apparatus for spark plasma sintering.

temperature was further increased to 950 °C within 1 min and held for 5 min. After this, the pulse current was cut and the applied pressure was released before allowing the system to cool down to room temperature. The sintered pellets (10 mm in diameter and 2 mm in thickness) were then removed and the graphite sheet adhering on the pellet was scraped off. The pellets were then annealed in air for 2 h at 900 °C to remove any residual carbon. The rate of heating and cooling in the heat treatment was maintained at 2 °C/min.

2.2. Characterization

The densities of the SPS-prepared samples were measured by the Archimedes method using distilled water. The phase purity and structure of the samples were evaluated by X-ray diffraction (XRD) using a Rigaku diffractometer with Cu-Kα radiation (D/max-RB, Rigaku Co., Tokyo, Japan) and an acceleration voltage of 40 kV and a beam current of 30 mA with a 2θ scanning step of 0.02° and a count time of 5 s. Microstructural features on the fracture surfaces of the samples were examined using field emission scanning electron microscopy (FE-SEM, Hitachi S-4700), from which the grain sizes in the samples were estimated using the linear intercept method [14].

The electrical permittivity measurements were performed using a computer controlled impedance analyzer (HIOKI 3535-50 LCR Hi Tester, Japan) with the maximum magnitude of 1 V at a fixed frequency of 100 kHz. Prior to the electrical measurements, the samples were coated with Au paste, cured at 120 °C for 2 h, and then poled in silicone oil at 150 °C under a dc field of 10 kV/cm for 2 h. This process ensured a balanced polarization process and enabled observation of any changes in piezoelectric properties. The dielectric properties of all samples were measured over the temperature range of 30–350 °C. Ferroelectric hysteresis measurements were performed at room temperature by virtue of an automatic PE loop tracer based on a Radiant Technologies ferroelectric test system (Radiant Technologies, Precision Premier, Precision Material Analyser, USA) with virtual ground mode at 1 kHz.

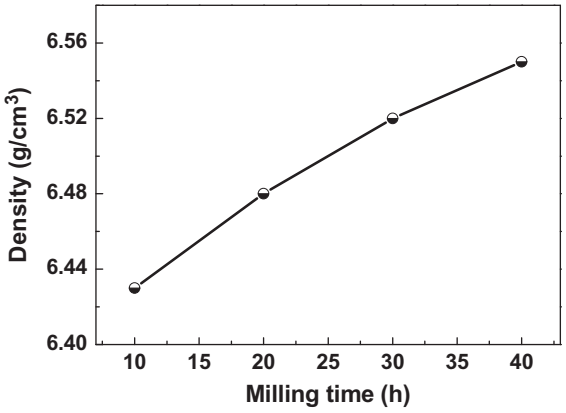

Fig. 2. The density as a function of ball milling time for the prepared $Ba_{0.8}Pb_{0.2}TiO_3$ ceramics.

3. Results and discussion

3.1. Densification

The bulk density of the SPS-prepared samples is plotted in Fig. 2 as a function of ball milling time. It can be seen that as the milling time is increased from 10 h to 40 h, the bulk density increases and reaches 6.55 g/cm^3, which is about 99% of the theoretical density. The theoretical density of the $Ba_{0.8}Pb_{0.2}TiO_3$ ceramic (6.57 g/cm^3) was calculated from its crystal structure and lattice parameters. Although the milling time is long, the SPS process is extremely short and takes only about 5 min to complete the process. Since the densities of the different samples are similar to each other, the difference in the electrical properties of the samples caused by the density difference should be very small.

Generally, sintering is a bulk diffusion-controlled mass transfer phenomenon and higher temperatures are expected to accelerate the diffusion kinetics and thereby improve densification. Ultimately, the diffusion and mass transfer stops as the driving force for further sintering is very small, and the densification will not be further improved with further increasing temperature or time, but grain growth may take place. However, in the case of nanoparticles, surface diffusion dominates the mass transfer which clearly enhances the densification process as seen for smaller particle sizes obtained by longer milling times.

3.2. Microstructural and crystallographic analyses

After SPS processing, the BPT compacts changed to a dark gray color from the white-colored precursor powder, and this can be attributed to carbon contamination from the die lining. Subsequent annealing of the as-prepared SPS samples in air at 900 °C enables carbon to be removed, making the color changed from dark gray to cream white. The presence of carbon before annealing and the subsequent removal by annealing were confirmed by energy dispersive X-ray micro-analysis. It is possible that the as-prepared SPS pellets became dark gray in color because of oxygen deficiency in their crystal lattice, which was caused by the reduced oxygen atmosphere in the SPS system. The oxygen deficiency could be supplemented during the annealing in air at 900 °C, making the color of the pellets become cream white. In order to minimize any volatilization of lead, a powder bed was used to provide a PbO-rich atmosphere and during annealing all the as-prepared SPS pellets were covered with the same composition powder by virtue of a closed double crucible. To confirm whether there was any Pb loss during annealing, energy dispersive X-ray spectroscopy (EDS) was performed on the fresh fracture surfaces of some 40 h-milled SPS-prepared samples. The results showed that the concentration of Pb was approximately 4 at%, indicating that there was no visible Pb loss in the samples (the calculated Pb content in $Ba_{0.8}Pb_{0.2}TiO_3$ is 4 at%).

Fig. 3 shows the FE-SEM images of the powders after ball milling for 10 h and 40 h, respectively. As seen, they both consist of more or less spherical particles. The particles are nano-sized for both conditions, but the powders milled for 40 h are apparently finer in comparison with those milled for 10 h. In addition, there is some agglomeration of the powders, especially for the 40 h-milled ones. The FE-SEM images of the fracture surfaces of the SPS-prepared samples in Fig. 4 show that the microstructure is quite uniform but increasingly dense

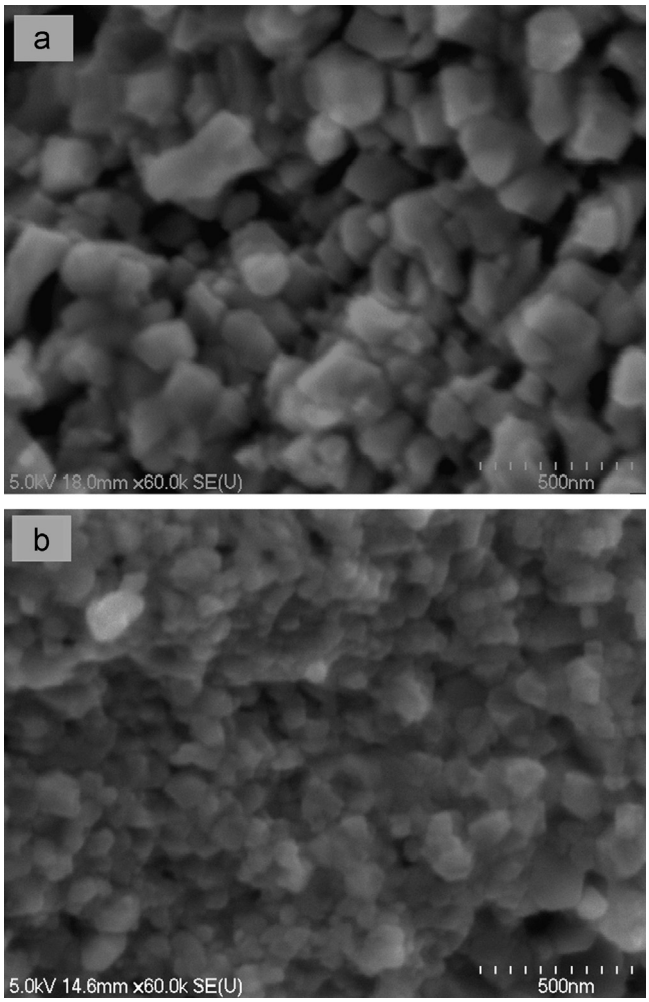

Fig. 3. FE-SEM morphologies of the powders after ball milling for (a) 10 h and (b) 40 h, respectively.

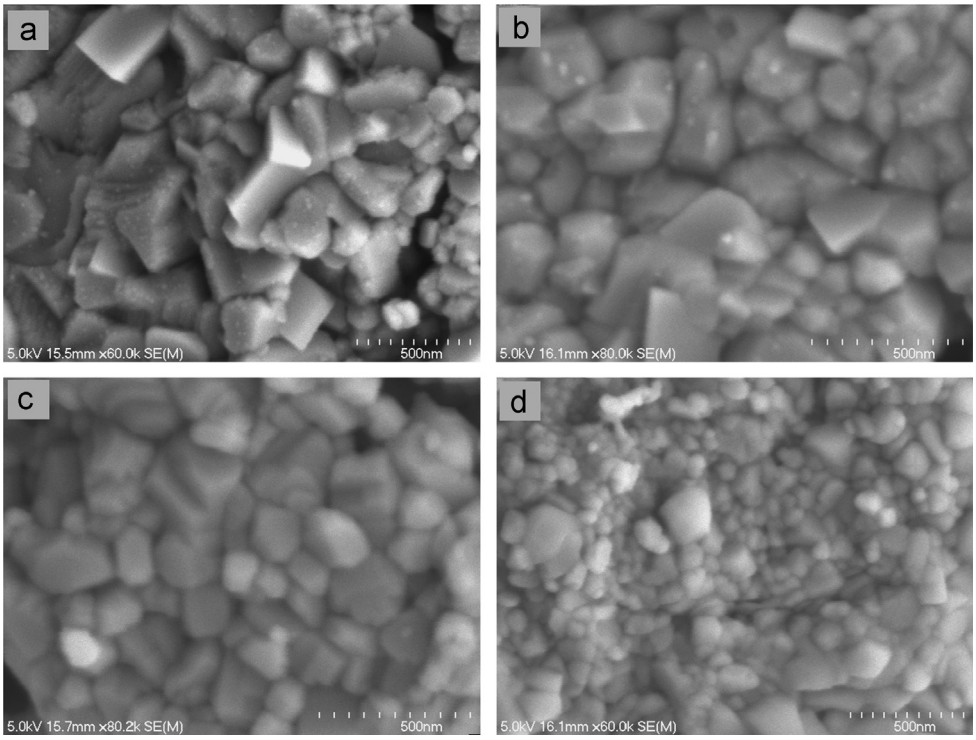

Fig. 4. FE-SEM images of the fracture surfaces of the $Ba_{0.8}Pb_{0.2}TiO_3$ ceramic samples prepared by the SPS with different milling times: (a) 10 h; (b) 20 h; (c) 30 h; and (d) 40 h.

with increasing milling time. As can be seen, the grain size decreases gradually and the average values in grain size are approximately 200 nm, 150 nm, 100 nm, and 60 nm for the samples with the milling times of 10, 20, 30 and 40 h, respectively.

The room temperature XRD patterns of the SPS-prepared BPT samples with different grain sizes are shown in Fig. 5a. All the samples show similar XRD profiles with the formation of tetragonal phase characterized by the splitting of (002) and (200) reflections as shown in Fig. 5b. Moreover, the intensity difference between (002) and (200) reflections increases with decreasing grain size. The indexing of XRD peaks and determination of lattice parameters of BPT were carried out using a software package POWD. On the basis of the best agreement between the observed and calculated *d* values of all the reflections, a unit cell of BPT was selected and its lattice parameters were refined using a least square subroutine of POWD. The lattice parameters *a* and *c* were obtained as 0.39324 and 0.40369 nm, 0.39336 and 0.40355 nm, 0.39339 and 0.40348 nm, and 0.39347 and 0.40332 nm, for the 10, 20, 30 and 40 h-milled and sintered samples, respectively. The lattice parameter *a* increases very slightly, while the lattice parameter *c* decreases very slightly with increasing milling time. Hence the *c*/*a* ratios for the four samples are close to each other, suggesting that the phase structure is similar to each other irrespective of the milling time.

3.3. Dielectric properties

Fig. 6a shows the temperature dependence (30–350 °C) of dielectric constant, measured at a fixed frequency of 100 kHz, for the SPS-prepared BPT ceramics. Clearly, in all the cases, the dielectric constant increases with increasing temperature and reaches a maximum value ε_{max} at ~225 °C, i.e. the Curie transition temperature (T_c), and then decreases with further increase in temperature. The dielectric peak is broad, which is a general feature for ferroelectric materials [15]. The dielectric constants at T_c are about 8000, 13,500, 15,700, and 19,000, corresponding to the average grain sizes of approximately 200, 150, 100, and 60 nm, respectively, confirming that the dielectric constant increases with decreasing grain size as shown in Ref. [16]. The maximum dielectric constant appears, as expected, at around 225 °C, which are corresponding to the Curie transition temperature of BPT, where the transition between the ferroelectric (crystallographic tetragonal polymorph) and the paraelectric (crystallographic cubic polymorph) occurs [17]. The Curie transition temperature (T_c) does not show significant variation and it is about 225 °C for all the four samples.

The temperature dependence of dielectric loss (tan δ) is shown in Fig. 6b. It can be seen that the value of tan δ remains very low until T_c, beyond which it shows an increase for the 10 h and 20 h-milled SPS samples, while a decrease occurs for the 30 h and 40 h-milled SPS samples. At T_c, the dielectric loss decreases with decreasing grain size with the values of 0.081, 0.078, 0.066, and 0.059 which are corresponding to the average grain sizes of 200, 150, 100, and 60 nm, respectively. A study by Arya et al. [6] has also shown the same phenomenon for a nano-sized barium lead titanate prepared through a citrate precursor route. The above results demonstrate that decreasing grain size is beneficial for the reduction of dielectric loss.

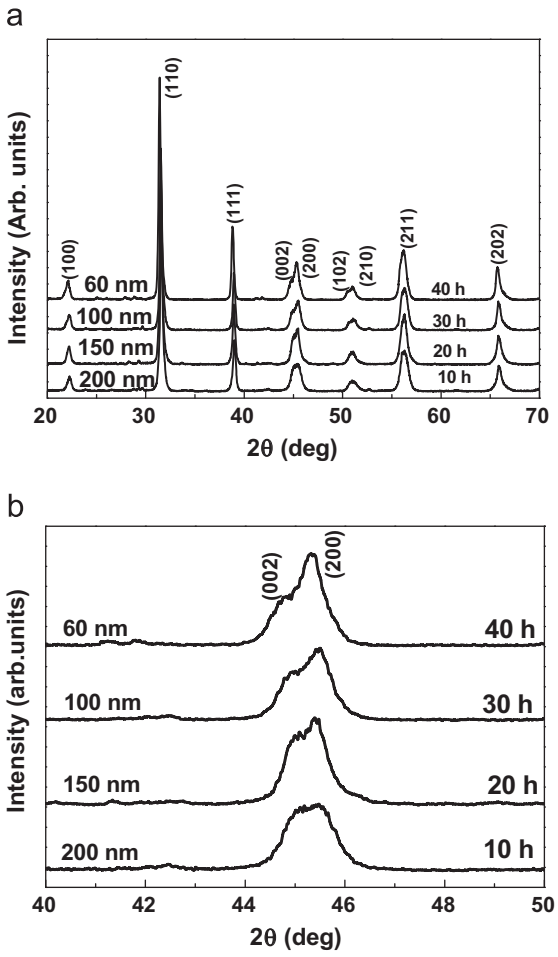

Fig. 5. (a) X-ray diffraction patterns (Cu-Kα radiation) for the prepared $Ba_{0.8}Pb_{0.2}TiO_3$ ceramics with different milling times (or grain sizes) and (b) detailed diffraction profiles around $2\theta=45^{o}$.

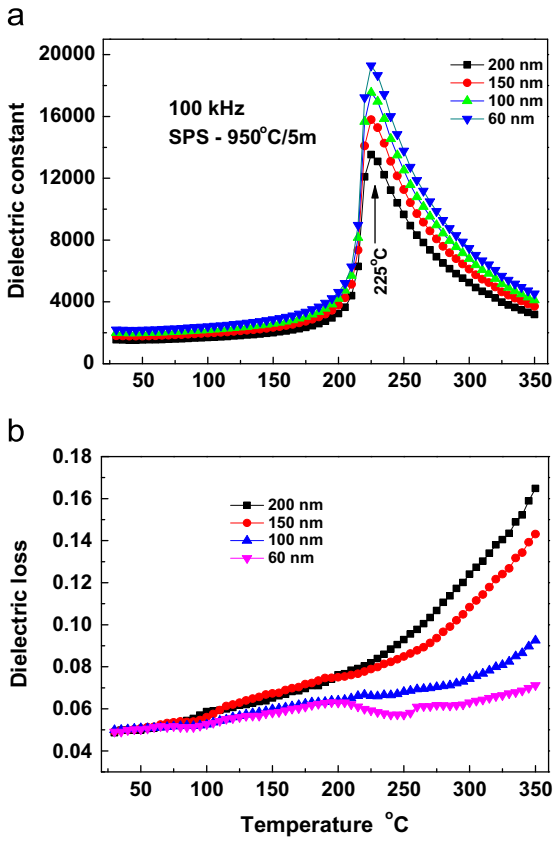

Fig. 6. Temperature dependences of (a) dielectric constant and (b) dielectric loss for the prepared $Ba_{0.8}Pb_{0.2}TiO_3$ ceramics with different grain sizes, measured at a frequency of 100 kHz.

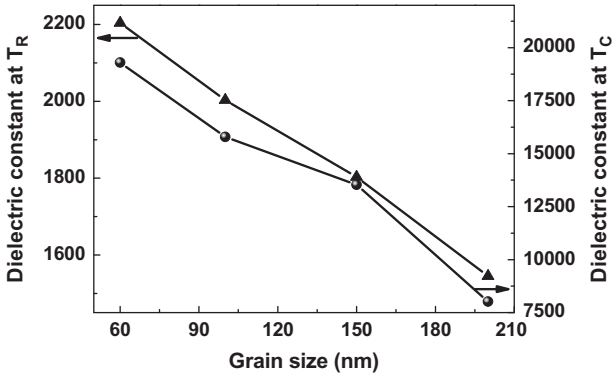

Fig. 7. Room temperature (T_R) and transition temperature (T_c) dielectric constants of the prepared $Ba_{0.8}Pb_{0.2}TiO_3$ ceramics as a function of grain size.

Dielectric constants at room temperature (T_R) and Curie temperature (T_c) as a function of the grain size of the SPS-prepared BPT are shown in Fig. 7. As can be seen, both the room temperature and Curie temperature dielectric constants increase with decreasing grain size. The large dielectric constant of the samples could be due to the nanocrystalline nature of the BPT by the synergistic effect of crystallite size [18]. The dielectric constant can also be analyzed using the molar polarizability (α_D) which may be evaluated by the Clausius–Mossotti relation [19,20]

$$\alpha_D = \frac{3V_m(\varepsilon_r - 1)}{4\pi(\varepsilon_r + 2)} \quad (1)$$

where V_m is the molar volume and ε_r is the dielectric constant. Since the lattice parameters, as shown above, are very close to each other for all the samples, the molar volume may be regarded as a fixed value. Owing to the fact that the dielectric constant increases with decreasing grain size, one can draw a plot between α_D and grain size with Eq. (1) along with the measured dielectric constants, which is shown in Fig. 8. Clearly, the polarizability increases somewhat with decreasing grain size. This implies that the ability for a BPT "molecule" to be polarized increases slightly with decreasing grain size in the present case.

Similar results and trends have been obtained by Parashar et al. [16,20] in PGZT and PNZT nanocrystalline ceramics. Their results show that the dielectric constant increases with decreasing crystallite size in both PGZT and PNZT polycrystals. The maximum dielectric constant in PGZT is 7296 for a grain size of 21 nm and 10,626 for a grain size of 30 nm, but as seen in Fig. 7 the value obtained in the present work is much higher than these values. Also, a study by Hungria et al.

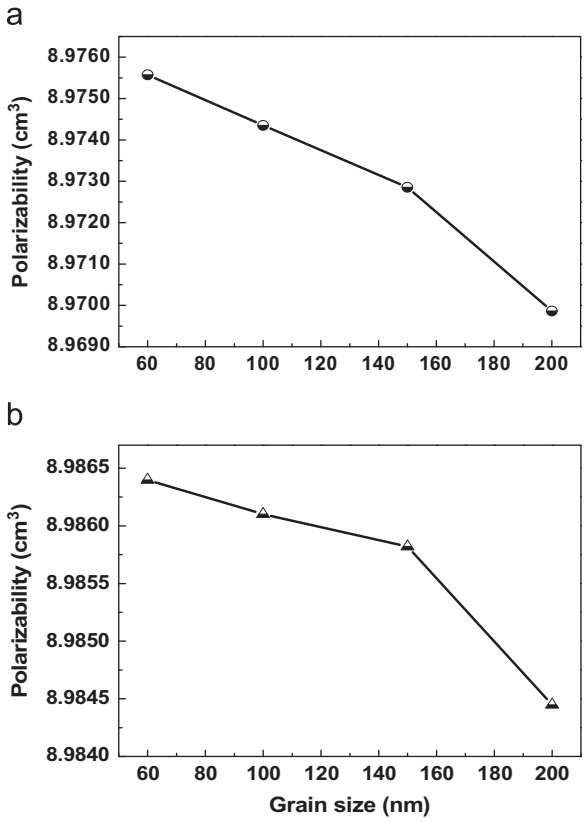

Fig. 8. Grain size dependence of the molar polarizability at (a) room temperature (T_R) and (b) transition temperature (T_c) for the prepared $Ba_{0.8}Pb_{0.2}TiO_3$ ceramics, determined with Eq. (1) along with the measured dielectric constants.

shows the same behavior in PZN-PT nanocrystalline ceramics prepared by mechanosynthesis and SPS [21].

In general, the electrical properties of ferroelectric ceramics increase with increasing grain size [22,23]. However this is not true in the present case because probably of nanosized-grain effects. The grain size in the BPT sample decreases with increasing milling time, which leads to an increase in dielectric constant. The nanosized- grain effect on the electrical properties could result from the domain-wall switching being restricted. As shown in Fig. 5b, the XRD intensity difference between (002) and (200) reflections increases with decreasing grain size. Usually, this difference is caused by a difference in domain size [24]. Since the domain size decreases with decreasing grain size [23], the intensity difference between (002) and (200) reflections increases with decreasing grain size. The increased domain density due to the decreased domain size could enhance the ionic polarizability as well as the orientational polarizability, as shown in Fig. 8, leading to a higher permittivity [24]. It is generally acknowledged that the internal electric dipoles are coupled to the lattice and thus the cubic – tetragonal 'distortion' may change the strength of the dipoles and result in a change in dielectric constant with decreasing grain size down to ~20 nm [25–28]. The higher value of ε_{max} with a finer grain size may in part be attributed to the pinning effect of the domain wall. When the crystallite size becomes comparable to the domain wall width, pinning may occur inside the grains and the domain wall motion may be inhibited. The reduction in the domain wall mobility may decrease the switching rate, thereby raising ε_{max}.

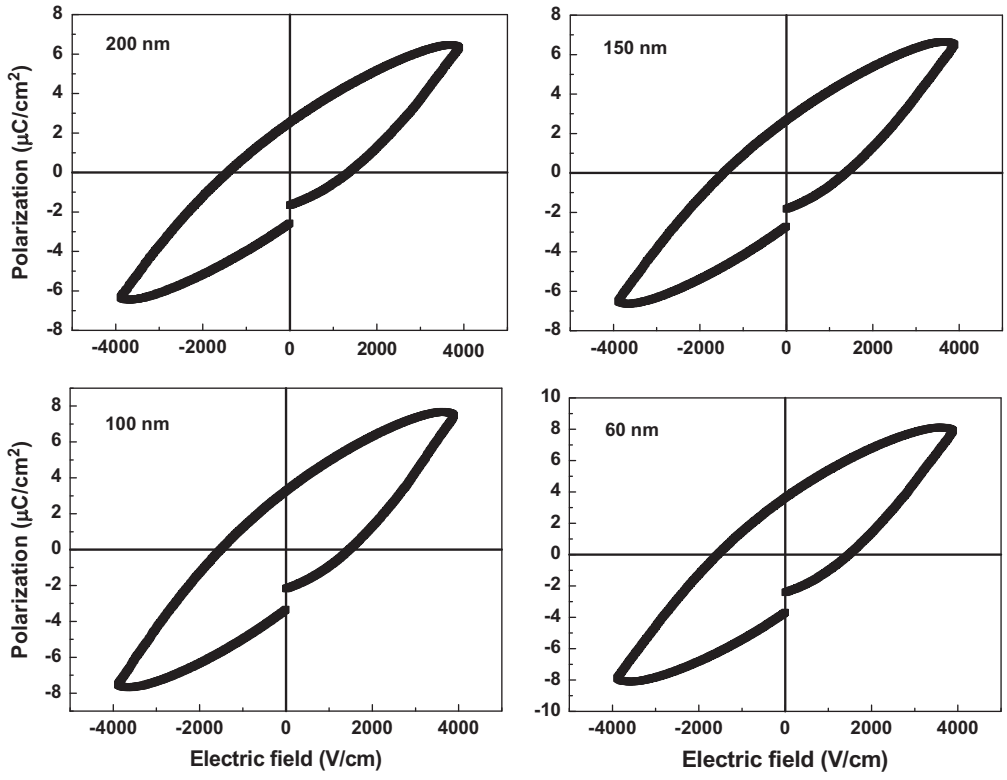

Fig. 9. Ferroelectric hysteresis loops for the prepared $Ba_{0.8}Pb_{0.2}TiO_3$ ceramics with different grain sizes, measured at room temperature.

3.4. P–E hysteresis loops

Fig. 9 shows the room temperature ferroelectric hysteresis loops of the SPS-prepared samples with different grain sizes. All the SPS-prepared samples possess a typical ferroelectric polarization hysteresis loop (P–E loop). The shape of the P–E loops is elliptical and it is not completely saturated possibly due to a small leakage current in the samples. The P–E loop shape may be affected by many factors including microstructure, charged defects, mechanical stress, preparation condition and thermal treatment [29]. Amorin et al. [30] also observed the same leakage behavior in the P–E loops of $BiScO_3$-$PbTiO_3$ nanocrystalline ceramics with an average grain size below 375 nm, prepared by mechanosynthesis and SPS. Furthermore, Chen et al. [31] found the same PE-loop behavior for the BST thin films with the grain size range of 250–650 nm.

The values of remanent polarization (P_r), spontaneous polarization (P_s) and coercive filed (E_c), determined from Fig. 9, are represented in Fig. 10. As can be seen, P_r, P_s and E_c all increase slightly with increasing grain size, as shown elsewhere [32]. For the sample with an average grain size of approximately 60 nm, P_r, P_s and E_c are 2.5 μC/cm^2, 6.3 μC/cm^2 and 1.34 kV/cm, respectively. Meanwhile, for the samples with the average grain sizes of approximately 100 nm, 150 nm and 200 nm, they are 2.6 μC/cm^2, 6.4 μC/cm^2 and 1.36 kV/cm, 3.2 μC/cm^2, 7.4 μC/cm^2 and 1.47 kV/cm, 3.6 μC/cm^2, 7.8 μC/cm^2 and 1.48 kV/cm, respectively. Hence, although the observed P_r, P_s and E_c decrease slightly with decreasing grain size, they are still acceptable even for a grain size of ~60 nm. The above variations of P_r, P_s and E_c with grain size are consistent with the reports by Liu et al. [33] for PZT and by Ma et al. [34] for the nano-domain $BaTiO_3$. Moreover, Amorin et al. [30] observed the same behavior in $BiScO_3$–$PbTiO_3$ nanocrystalline ceramics prepared by mechanosynthesis and SPS. In their results, both spontaneous and remanent polarization values decrease continuously as the grain size decreases from 375 nm to 28 nm.

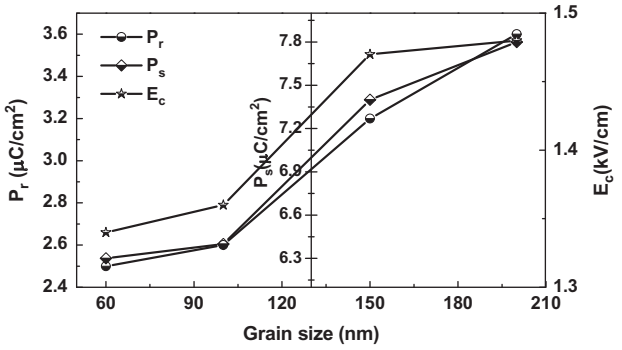

Fig. 10. Remanent polarization (P_r), spontaneous polarization (P_s) and coercive field (E_c) as a function of grain size for the prepared $Ba_{0.8}Pb_{0.2}TiO_3$ ceramics, determined from Fig. 9.

Grain size effects have been examined for ferroelectrics in the form of powders, composite materials, ceramics, and films [13,34,35]. The results from these studies indicate that the mechanisms of the grain size effect in isolated particles, particles embedded in a nonferroelectric matrix, grains in ceramics, and thin films are quite different. Nevertheless, ceramics seem to be a more convenient system to study the grain size effect, in comparison to powders and thin films for average isotopic characteristics. According to Zhao et al. [13], the causes for the size effect usually include the defect, hydroxyl, porosity, residual stress, boundary condition, and so on. Based on the results presented here, for the SPS-prepared high density nanocrystalline $Ba_{0.8}Pb_{0.2}TiO_3$ ceramics, the electrical properties are strongly dependent on the grain size. The various properties of the SPS-prepared ceramics are summarized in Table 1 from which one can see the effect of grain size on the electrical properties of the ceramics.

Finally, it is worth mentioning that the 40 h ball milling seems too long from the standpoint of energy impact and particle agglomeration. Consequently, in order to reduce energy consumption and particle agglomeration, it is necessary to shorten, to some degree, the ball milling time in engineering practice. Of course, the resulting particles will be somewhat larger as compared with the 40 h-milled ones, so that the dielectric constants of the resulting SPS samples will be somewhat lower (see Fig. 7).

4. Conclusions

Dense $Ba_{0.8}Pb_{0.2}TiO_3$ nanocrystalline ferroelectric ceramics have been successfully synthesized using SPS. It is confirmed from X-ray diffraction that all the ceramics possess a perovskite structure. As the ball milling time is increased from 10 h to 40 h, the average grain size of the sample decreases

Table 1
Comparison of crystallite size, lattice parameters, density (ρ), room temperature and transition temperature dielectric data (ε_{TR} and ε_{max}), dielectric loss tanδ, coercive field (E_c), remanent polarization (P_r), and spontaneous polarization (P_s) for the prepared $Ba_{0.8}Pb_{0.2}TiO_3$ ceramics

Parameters	Properties			
Grain size (nm)	~200	~150	~100	~60
a (nm)	0.39324	0.39336	0.39339	0.39347
c (nm)	0.40369	0.40355	0.40348	0.40332
c/a	1.0265	1.0259	1.0256	1.0250
ρ (g/cm^3)	6.43	6.48	6.52	6.55
ε_{TR}	1500	1800	2000	2200
ε_{max}	8000	13,500	15,700	19,000
tan δ at T_c	0.081	0.078	0.066	0.059
E_c (kV/cm)	1.48	1.47	1.36	1.34
P_r (μC/cm^2)	3.6	3.2	2.6	2.5
P_s (μC/cm^2)	7.8	7.4	6.4	6.3

from ~200 to ~60 nm. Both the room temperature and Curie transition temperature dielectric constants increase considerably with decreasing grain size. The 40 h-milled SPS sample (average grain size = ~60 nm) has the highest value of dielectric constant (19,000 at 225 °C). All the samples show a ferroelectric hysteresis loop and the values of P_r, P_s and E_c decrease slightly with decreasing grain size.

Acknowledgments

This work was supported by the National Natural Science Foundation of China under Grant no. 51171117 and the Science and Technology Foundation of Shenzhen.

References

[1] N. Setter, R. Waser, Electroceramic Materials, Acta Materialia 48 (2000) 151–178.
[2] W. Jillek, W.K.C. Yung, Embedded components in printed circuit boards: a processing technology review, International Journal of Advanced Manufacturing Technology 25 (2005) 350–360.
[3] M.H. Frey, D.A. Payne, Grain-size effect on structure and phase transformations for barium titanate, Physical Review B 54 (1) (1996) 3158–3168.
[4] D. Hennings, G.J. Rosenstin, Temperature-stable dielectrics based on chemically inhomogeneous $BaTiO_3$, Journal of the American Ceramic Society 67 (4) (1984) 249–254.
[5] M. Wangmann, R. Bronnimann, F. Clemens, T. Graule, Barium titanate-based PTCR thermistor fibers: processing and properties, Sensors and Actuators A 135 (2007) 394–404.
[6] P.R. Arya, P. Jha, G.N. Subbanna, A.K. Ganguli, Polymeric citrate precursor route to the synthesis of nano-sized barium lead titanates, Materials Research Bulletin 38 (2003) 617–628.
[7] C. Ma, H. Guo, S. Beckman, X. Tan, Breakthrough in understanding piezoelectric mechanism in Pb-Free ferroelectrics, American Ceramic Society Bulletin 91 (8) (2012) 16.
[8] C. Zhou, W.F. Liu, D.Z. Xue, X.B. Ren, H.X. Bao, J.H. Gao, L.X. Zhang, Triple-point-type morphotropic phase boundary based large piezoelectric Pb-free aterial-$Ba(Ti_{0.8}Hf_{0.2})O_3$-$(Ba_{0.7}Ca_{0.3})TiO_3$, Applied Physics Letters 100 (2012) 222910–222915.
[9] R.E. Vold, R. Biederman, G.A. Rossetti Jr, A. Sacco Jr, T. Sjodin, A. Rzhevskii, Hydrothermal synthesis of lead doped barium titanate, Journal of Materials Science 36 (2001) 2019–2026.
[10] M. Mastubara, T. Yamaguchi, W. Sakamoto, K. Kikuta, T. Yogo, S.I. Hirano, Processing and piezoelectric properties of lead free (K,Na) $(Nb,Ta)O_3$ ceramics, Journal of the American Ceramic Society 88 (5) (2005) 1190–1196.
[11] M. Mastabura, K. Kikuta, S.I. Hirano, Piezoelectric properties of $(K_{0.5}Na_{0.5})(Nb_{1-x}Ta_x)O_3$–$K_{5.4}CuTa_{10}O_{29}$ ceramics, Journal of Applied Physics 97 (2005) 114105–114107.
[12] R.E. Jaeger, L. Egerton, Hot pressing of potassium-sodium niobates, Journal of the American Ceramic Society 45 (5) (1962) 209–213.
[13] Z. Zhao, V. Buscaglia, M. Viviani, M.T. Buscaglia, L. Mitoseriu, A. Testino, M. Nygren, M. Johnsson, P. Nanni, Grain-size effects on the ferroelectric properties behavior of dense nanocrystalline $BaTiO_3$ ceramics, Physical Review B 70 (2007) 024107–024108.
[14] L.C. Stearns, M.P. Harmer, Particle-inhibited grain growth in Al_2O_3-SiC: I, experimental results, Journal of the American Ceramic Society 79 (12) (1996) 3013–3019.
[15] L. Mitoseriu, C. Harnagea, P. Nanni, A. Testino, M.T. Buscaglia, V. Buscaglia, M. Viviani, Z. Zhao, M. Nygren, Local switching properties of dense nanocrystalline $BaTiO_3$ ceramics, Applied Physics Letters 84 (13) (2004) 2418–2420.
[16] S.K.S. Parashar, R.N.P. Choudhary, B.S. Murty, Ferroelectric phase transition in $Pb_{0.92}Gd_{0.08}(Zr_{0.53}Ti_{0.47})_{0.98}O_3$ nanoceramic synthesized by high-energy ball milling, Journal of Applied Physics 94 (9) (2003) 6091–6096.
[17] M.G. Harwood, P. Popper, D.F. Rushman, Curie point of barium titanate, Nature 160 (1947) 58–59.
[18] Venkata Ramana Mudinepalli, B.S. Shenhua Song, Murty, effect of microwave sintering on structural and dielectric properties of $Ba_{1-x}(Sr/Pb)_xTiO_3$ ($x = 0.2$ for Sr and Pb) nanocrystalline ferroelectric ceramics, Journal of Materials Science: Materials in Electronics 24 (2013) 2141–2150.
[19] R.S. Hawke, R.N. Keeler, A.C. Mitchell, Microwave dielectric constant of Al_2O_3 at 375 Kilobars, Applied Physics Letters 14 (1969) 229–231.
[20] S.K.S. Parashar, R.N.P. Choudhary, B.S. Murty, Size effect of $Pb_{0.92}Nd_{0.08}(Zr_{0.53}Ti_{0.47})_{0.98}O_3$ nanoceramic synthesized by high-energy ball milling, Journal of Applied Physics 98 (2005) 104305–104308.
[21] T. Hungria, H. Amorin, J. Ricote, M. Alguero, A. Castro, Nanostructured ceramics of $0.92PbZn_{1/3}Nb_{2/3}O_3$-$0.08PbTiO_3$ processed by SPS of nanocrystalline powders by mechanosynthesis, Nanotechnology 19 (2008) 155609–155614.
[22] K. Okazaki, K. Nagata, Effect of Grain size and porosity on electrical and optical properties of PLZT ceramics, Journal of the American Ceramic Society 56 (2) (1973) 82–86.
[23] C.A. Randall, N. Kim, J.P. Kucera, W. Cao, T.R. Shrout, Intrinsic and extrinsic size effects in fine-grained morphotropic phase boundary lead zirconate titanate ceramics, Journal of the American Ceramic Society 81 (3) (1998) 677–688.
[24] T. Hoshina, K. Takizawa, J. Li, T. Kasama, H. Kakemoto, T. Tsurumi, Domain size effect on dielectric properties of barium titanate ceramics, Japanese Journal of Applied Physics 47 (2008) 7607–7611.
[25] W. Kanzig, Space charge layer near the surface of a ferroelectric, Physical Review 98 (1955) 549 (500).
[26] K. Ishikawa, K. Yoshikawa, N. Okada, Size effects on the ferroelectric phase transition in $PbTiO_3$ ultrafine particles, Physical Review B 37 (1988) 5852–5855.
[27] K. Uchino, E. Sadanaga, T. Hirose, Dependence of the crystal structure on particle size in barium titanate, Journal of the American Ceramic Society 72 (8) (1989) 1555–1561.
[28] A.Q. Jiang, G.H. Li, L.D. Zhang, Dielectric study in nanocrystalline $Bi_4Ti_3O_{12}$ prepared by chemical coprecipitation, Journal of Applied Physics 83 (1998) 4878–4883.
[29] D. Damjanovic, Ferroelectric, dielectric and piezoelectric properties of ferroelectric thin films and ceramics, Reports on Progress in Physics 61 (1998) 1267–1324.
[30] H. Amorin, R. Jimenez, J. Ricote, T. Hungria, A. Castro, M. Alguero, Apparent vanishing of ferroelectricity in nanostructured $BiScO_3$-$PbTiO_3$, Journal of Physics D: Applied Physics 43 (2010) 285401–285405.
[31] H. Chen, C. Yang, C. Fu, L. Zhao, Z. Gao, The size effect of $Ba_{0.6}Sr_{0.4}TiO_3$ thin films on the ferroelectric properties, Applied Surface Science 252 (2006) 4171–4177.
[32] H.S. Nalwa, Low and High Dielectric Constant Materials and their Applications, Academic Press, New York, 1999.
[33] J.S. Liu, S.R. Zhang, H.Z. Zeng, C.T. Yang, Y. Yuan, Coercive field dependence of the grain size of ferroelectric films, Physical Review B 72 (17) (2005) 172101–172103.
[34] N. Ma, B.-P. Zhang, W.-G. Yang, D. Gua, Phase structure and nano-domain in high performance of $BaTiO_3$ piezoelectric ceramics, Journal of the European Ceramic Society 32 (2012) 1059–1066.
[35] S. Tsunekawa, S. Ito, T. Mori, K. Ishikawa, Z.-Q. Li, Y. Kawazoe, Critical size and anomalous lattice expansion in nanocrstalline $BaTiO_3$ particles, Physical Review B 62 (2000) 3065–3070.